On the Performance of Roadside Unit-Assisted Energy Harvesting Full-Duplex Amplify-and-Forward Vehicle-to-Vehicle Relay Systems

Ba Cao Nguyen[a,b], Xuan Nam Tran[b], Le The Dung[c,d,*]

[a] *Faculty of Basic Techniques, Telecommunications University, Vietnam*
[b] *Advanced Wireless Communications Group, Le Quy Don Technical University, Vietnam*
[c] *Division of Computational Physics, Institute for Computational Science, Ton Duc Thang University, Ho Chi Minh City, Vietnam*
[d] *Faculty of Electrical and Electronics Engineering, Ton Duc Thang University, Ho Chi Minh City, Vietnam*

Abstract

This paper considers the performance of a full-duplex (FD) vehicle-to-vehicle (V2V) relay system where the relay uses amplify-and-forward (AF) protocol and harvests the energy from the radio frequency (RF) signals transmitted by source. Unlike previous reports, we investigate the case that both relay and destination are moving vehicles. Therefore, the channel between source and relay is Rayleigh fading while the channel between relay and destination is cascade (double) Raleigh fading. In addition, both fixed and variable gains are used at the FD relay. Based on mathematical analysis, we successfully derive the exact closed-form expressions of the outage probability (OP) and symbol error probability (SEP) to evaluate the system performance. Monte-Carlo simulations are exploited to demonstrate the correctness of all derived mathematical expressions. Numerical results clearly indicate that the OP and SEP performance of the considered energy harvesting (EH)-FD-V2V relay system with variable gain is much better than that with fixed gain. Moreover, the OP and SEP performance are strongly impacted by residual self-interference (RSI) due to the incomplete noise cancellation during the FD transmission. Besides the RSI, the OP and SEP performance is greatly reduced because of the cascade Rayleigh fading. We also observe that there is an optimal EH time duration to minimize the OP and SEP and this optimal value is different for fixed and variable gains. Therefore, from the transmission power of source and the type of gains used at FD relay, we can choose a suitable time EH time duration to get the best system performance.

Keywords: vehicle-to-vehicle communication, energy harvesting, full-duplex relay, cascade Raleigh fading, outage probability, symbol error probability.

1. Introduction

In the age of the Internet of Things (IoT) devices, the number of smartphones is rapidly increased with various functions such as in health-care, controlling machines, and other missions such as for smart home, automatic driving. Therefore, the requirements of low energy consumption and spectral efficiency usage become a hot topic for both researches and implementations [1–3]. There have been many solutions such as using low power consumption devices, harvesting energy from radio frequency (RF) signals proposed to maintain the operation of wireless devices. Recently, applying energy harvesting (EH) technique for wireless devices has becomes a promising solution because

*Corresponding author
Email address: lethedung@tdtu.edu.vn (Le The Dung)

these devices always move during their operations, especially for personal devices. In addition, it was demonstrated in [4] that integrating of simultaneous wireless information and power transfer (SWIPT) into typical fifth generation (5G) systems including IoTs, device-to-device (D2D) networks, HetNets, and cognitive radio networks (CRNs) can bring benefits in improving energy and spectral efficiency. Especially, SWIPT provides a great solution for the extremely remote area communication (eRAC) where mobile edge devices can be located outside the coverage of the electric grid for reasons such as deployment constraints, reliability requirements, weather, disasters, and maintenance expenses. Besides EH, full-duplex (FD) technique can double the capacity of wireless systems because FD devices can simultaneously transmit and receive signals by using the same temporal and frequency resources [3, 5, 6]. Therefore, FD communication systems have been widely employed in practice, including the IoT applications [7, 8].

In the literature, the usage of FD communication in relay networks has been exploited in various scenarios because of the benefits of both FD and relay communications [6, 9–13]. It was showed that FD relay systems significantly improve the capacity of the systems compared with the traditional half-duplex (HD) relay systems, especially when several methods such as pilot optimization, power allocation, high-performance beamformer, and low-complexity detector are applied [12, 13]. However, the residual self-interference (RSI) induced by the FD communication substantially impacts the performance of FD relay systems. The RSI reduces not only bit error rate (BER) performance but also the capacity of FD relay systems. Fortunately, thanks to the fast development of antenna and circuit designs combining with various signal processing methods in both analog and digital domains, the RSI power can be decreased to the noise floor, making FD relay system feasible to implement in wireless systems [14–16]. The FD devices can be used in many applications of vehicle-to-vehicle (V2V) communications [3]. Since FD devices reduce the end-to-end transmission delay of communication between vehicles, it can use for intelligent transportation systems (ITS) [17–19]. The performance of FD-V2V relay systems was studied in [17, 19], where both decode-and-forward (DF) and amplify-and-forward (AF) schemes over cascade Rayleigh fading were considered. It was indicated that the performance of FD-V2V relay system is significantly reduced in comparison with that system over other channels such as Rayleigh fading. Furthermore, the impacts of both RSI and the cascade Rayleigh fading are stronger in high signal-to-noise ratio (SNR) regime, making the OP and SEP of FD-V2V relay system go to the error floor. Thus, various solutions such as antenna design [20], and interference management [21] have been proposed to mitigate the effects of RSI and cascade Rayleigh fading.

Combining EH and FD relay into wireless systems has been studied in many works, such as [14, 22–24]. In EH-FD relay systems, either FD relay harvests energy through RF signals transmitted from source [14, 24] or both source and FD relay harvest energy through RF signals transmitted from power beacon (PB) [22, 23]. Through mathematical analysis, these papers derived the exact expressions of outage probability (OP) and symbol error probability (SEP) of the EH-FD relay systems. Their results showed that the RSI significantly reduces the OP and SEP performance of the EH-FD relay systems. Furthermore, the usage of PB with multiple antennas can dramatically improve the OP and SEP performance because the RF signals from the PB often have higher energy than the RF signals from the source. Moreover, for a specific transmission power of PB or source, there is an optimal EH time duration that minimizes the OP and SEP of the EH-FD relay systems. In addition, EH and FD techniques were now combined with other new techniques such as non-orthogonal multiple access (NOMA) in [25]

to enhance the spectrum. On the other hand, a new secrecy information and energy transfer scheme for EH-FD systems were proposed in [26, 27]. Through the achievable secrecy rate obtained by numerical analysis, the optimal methods such as jointly optimizing the energy and information beamforming vectors [26], nonconvex optimization problem [27] are applied to to maximize the secrecy rate of the systems.

Recently, the combination of EH and FD techniques in V2V communication systems has become an inevitable trend for the fifth-generation (5G) and beyond (B5G) wireless networks. Due to the fact that EH from RF signals has great potential to provide stable energy to low-power energy-constrained networks including wireless sensor networks (WSNs), IoTs, and eRAC use cases in 5G and B5G networks [4, 28, 29]. Meanwhile, FD communications is expected to support a set of safety applications which make vehicles aware of road hazards or hidden objects [3]. It is because FD communications can help to solve some important problems in existing wireless networks, such as feedback delay and end-to-end delay reduction, network secrecy and efficiency improvement, increasing the spectrum usage flexibility and throughput, collision avoidance, solving the hidden terminal problem, reducing congestion with the aid of medium access layer (MAC) scheduling [3, 30]. Moreover, because of the moving of wireless devices in V2V communication systems, the traditional channels between nodes such as Rayleigh, Rician, and Nakagami-m fading channels may not be suitable. Instead, both theoretical analyses and practical measures have shown that the cascade Rayleigh fading channels are ideal for V2V communication systems [31–33]. However, when the cascade Rayleigh fading channels are considered in V2V communication systems, the calculation complexity will increase, leading to the difficulty in mathematically evaluating the performance of V2V communication systems, especially for the EH-V2V communication systems.

Motivated by the above issues, to exploit the benefits of both EH and FD relay techniques in V2V communication systems, we study a system where EH, FD relay are exploited in the scenario of V2V communication. In the considered EH-FD-V2V relay system, the source is a static roadside unit while both relay and destination are vehicles. Furthermore, the relay is powered by RF signals from source to support data transmission. So far, this is the first work considering EH and FD relay in the V2V communication system. With the fast development of circuit design, analog and digital signal processing in recent years and forecast of the future, the considered scenario can be successfully exploited in crucial vehicular scenarios such as in vehicle-to-roadside (V2R) communications, V2V interactions for safety applications. The contributions of this paper can be summarized as follows:

– We investigate an EH-FD-V2V relay system where the source is stationary while relay and destination are mobile. This assumption leads to the channel from source to relay is Rayleigh fading channel while the channel from the relay to the destination is cascade Rayleigh fading channels. Moreover, relay is powered from the source through RF signals to support data transmission. We consider two kinds of gain, i.e., fixed and variable gains at the FD relay.

– We successfully obtain the exact closed-form expressions of OP and SEP of the considered EH-FD-V2V relay system over cascade Rayleigh fading channels and under the effect of RSI due to FD transmission mode for both cases of fixed and variable gains. Based on the expression of OP, we also calculate the throughput of the considered EH-FD-V2V relay system. All analysis expressions are validated via Monte-Carlo simulations.

– We evaluate the performance of EH-FD-V2V relay system in various scenarios. Numerical results clearly indicate that the performance with variable gain is much better than that with fixed gain. Moreover, the RSI has

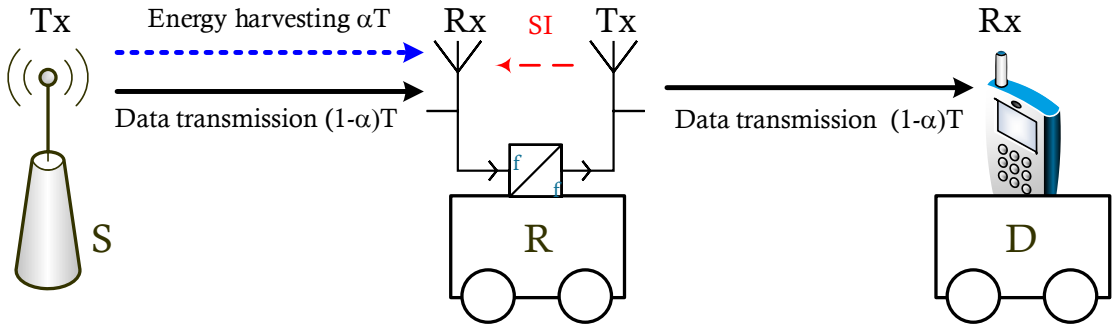

Figure 1: Illustration of the considered EH-FD-V2V relay system.

a substantial impact on the OP and SEP of the considered system for both cases fixed and variable gains. The performance of the EH-FD-V2V relay system is reduced compared with this system over Rayleigh fading channels. Also, for specific transmission power of the source, there is an optimal value of EH time duration that minimizes OP of the considered system, and this optimal value of fixed gain is different from that of variable gain.

The rest of this paper is organized as follows. Section 2 presents the system and signal model of the considered EH-FD-V2V relay system. Section 3 derives the mathematical expressions of the OP and SEP of the considered system. Section 4 provides numerical results and discussions. Finally, Section 5 concludes the paper.

2. System Model

The system model of the considered EH-FD-V2V relay system includes three nodes: source (S), relay (R), and destination (D) as illustrated in Fig. 1. In this system, S is static roadside unit while R and D are moving vehicles. S and D have only one antenna and operate in HD mode. Meanwhile, R has two antennas, one for transmitting and another for receiving and operates in FD mode. Data is transferred from S to D via the assistance of R. Furthermore, since the power supply of R is limited, when R moves on the road and exchanges data for a long time, it harvests the energy from RF signals transmitted by S to support the data transmission. To perform this task, R has a suitable energy harvester and a superior capacitor to store the harvested energy. Moreover, it is assumed that all harvested energy of R is used for data transmission in one symbol period.

The operation of the considered EH-FD-V2V relay system is comprised of two stages: EH and data transmission. Let us denote T as the time duration of an entire transmission block. The first time duration, αT, is used for EH while the remaining time duration, $(1-\alpha)$T, is used for data transmission, where α, $0 \leqslant \alpha \leqslant 1$, represents the time switching ratio and . Due to the FD mode, i.e., R simultaneously transmits signals to D and receives signals from S at the same time and on the same frequency band, the SI from transmitting antenna to the receiving antenna occurs. Therefore, all SIC techniques such as antenna domain suppression, analog and digital domain cancellation need to be exploited at R to reduce the SI effect. Since R uses a separate antenna for signal transmission and reception, it can easily apply all SI suppressing methods in antenna domain such as isolation, cross-polarization, and antenna directionality [34]. Although, a shared-antenna with a circulator can be used at R, the usage of a separate antenna can provide better SI suppression compared with shared-antenna [3, 10, 34].

During the time duration αT for EH, the harvested energy at R (denoted by E_h^{R}) is expressed as [35][1]

$$E_h^{\mathrm{R}} = \eta\alpha \mathrm{T} P_{\mathrm{S}} |h_{\mathrm{SR}}|^2, \tag{1}$$

where η, $0 \leqslant \eta \leqslant 1$, is the energy conversion efficiency; P_{S} is the average transmission power of S; h_{SR} is the fading coefficient of S – R channel. For any energy harvester, the energy conversion efficiency is constant and depends on the quality of electric circuitry. It should be noticed that R can use two antennas for EH to increase the harvested energy. However, higher harvested energy leads to higher transmission power at R and thus higher SI power. As a result, the OP and SEP performance of the system is reduced compared with the case of using only one antenna for EH [38]. Therefore, we consider the case of only one antenna is used at R for EH.

Since all harvested energy at R is used for the data transmission, the transmission power of R is expressed as

$$P_{\mathrm{R}} = \frac{\eta\alpha \mathrm{T} P_{\mathrm{S}} |h_{\mathrm{SR}}|^2}{(1-\alpha)\mathrm{T}} = \frac{\eta\alpha P_{\mathrm{S}} |h_{\mathrm{SR}}|^2}{1-\alpha}. \tag{2}$$

Next, during the time duration $(1-\alpha)$T, the data are transmitted from S to R and from R to D simultaneously, causing the SI from transmission antenna to reception antenna of R. Consequently, the received signals at R is given by

$$y_{\mathrm{R}} = h_{\mathrm{SR}} \sqrt{P_{\mathrm{S}}} x_{\mathrm{S}} + \tilde{h}_{\mathrm{RR}} \sqrt{P_{\mathrm{R}}} x_{\mathrm{R}} + z_{\mathrm{R}}, \tag{3}$$

where h_{SR} and $\tilde{h}_{\mathrm{RR}}$ are the fading coefficients of the channels from S to R and from the transmission antenna to the reception antenna of R, respectively; P_{S} and P_{R} are respectively the average signal transmission power of S and R; x_{S} and x_{R} are the transmitted signals at S and R, respectively; z_{R} is the Gaussian noise with zero-mean and variance of σ^2, i.e., $z_{\mathrm{R}} \sim \mathcal{CN}(0, \sigma^2)$. We should note that the term $\tilde{h}_{\mathrm{RR}} \sqrt{P_{\mathrm{R}}} x_{\mathrm{R}}$ is the SI due to FD mode and its average power before SIC is calculated as

$$\mathbb{E}\{|\tilde{h}_{\mathrm{RR}}|^2 P_{\mathrm{R}}\} = \frac{\eta\alpha P_{\mathrm{S}}}{1-\alpha} \mathbb{E}\left\{|\tilde{h}_{\mathrm{RR}}|^2 |h_{\mathrm{SR}}|^2\right\}, \tag{4}$$

where $\mathbb{E}\{.\}$ is the expectation operator.

As aforementioned, all SIC techniques such as antenna propagation, analog suppression, and digital cancellation must be applied at R to reduce the SI power. Particularly, R knows its transmitted signals, and it can subtract SI from the received signal via SI channel estimation, especially in digital domain cancellation [16, 22, 39, 40]. However, due to the imperfect channel estimation and the imperfect hardware of cancellation circuits, R cannot completely remove the SI from the received signals. Thus, the residual SI (RSI) still exists at R. Furthermore, the

[1] It is noted that, in practical scenario, the output power of EH circuit may depend on a certain saturation power threshold P_{th}. Specifically, if the input power exceeds P_{th}, the output power remains unchanged. This nonlinear characteristic of energy harvester are caused by various factors such as diode and saturation nonlinearities. Researches and experiments have demonstrated that the saturation nonlinearities of energy harvesting circuits cannot avoid in realistic systems [36, 37]. As a result of this fact, the harvested energy at R with nonlinear energy harvester can be obtained by extending (1) as

$$E_h^{\mathrm{R}} = \begin{cases} \eta\alpha \mathrm{T} P_{\mathrm{S}} |h_{\mathrm{SR}}|^2, & P_{\mathrm{S}} |h_{\mathrm{SR}}|^2 \leq P_{\mathrm{th}}, \\ \eta\alpha \mathrm{T} P_{\mathrm{th}}, & P_{\mathrm{S}} |h_{\mathrm{SR}}|^2 > P_{\mathrm{th}}. \end{cases}$$

RSI (denoted by $I_{\rm R}$) follows complex Gaussian distribution with zero mean and variance of $\gamma_{\rm RSI}$ [15, 16, 22, 41], where $\gamma_{\rm RSI}$ is

$$\gamma_{\rm RSI} = \frac{k\eta\alpha P_{\rm S}}{1-\alpha}, \tag{5}$$

with k denotes the SIC capability of the FD relay.

Then, we can rewrite (3) as

$$y_{\rm R} = h_{\rm SR}\sqrt{P_{\rm S}}x_{\rm S} + I_{\rm R} + z_{\rm R}. \tag{6}$$

After doing SIC, R amplifies the received signal before forwarding it to D. Therefore, the transmitted signal from R is expressed as

$$x_{\rm R} = Gy_{\rm R}, \tag{7}$$

where G is the relaying gain.

In the case that R knows the channel state information (CSI) of S – R channel, it uses variable gain ($G_{\rm v}$). Otherwise, it uses fixed gain ($G_{\rm f}$). These gains are computed subject to the normalized transmission power of R, i.e.,

$$G_{\rm f} = \sqrt{\frac{1}{\Omega_1 P_{\rm S} + \gamma_{\rm RSI} + \sigma^2}}, \tag{8}$$

$$G_{\rm v} = \sqrt{\frac{1}{|h_{\rm SR}|^2 P_{\rm S} + \gamma_{\rm RSI} + \sigma^2}}. \tag{9}$$

where $\Omega_1 = \mathbb{E}\{|h_{\rm SR}|^2\}$ is the average channel gain of S – R channel.

In this paper, we normalize all average channel gains, i.e., $\Omega_1 = 1$ for all channel gains. Therefore, the fixed gain now becomes

$$G_{\rm f} = \sqrt{\frac{1}{P_{\rm S} + \gamma_{\rm RSI} + \sigma^2}}. \tag{10}$$

The received signal at D is given by

$$y_{\rm D} = h_{\rm RD}\sqrt{P_{\rm R}}x_{\rm R} + z_{\rm D}, \tag{11}$$

where $h_{\rm RD}$ is the fading coefficient of R – D channel; $z_{\rm D}$ is the Gaussian noise at D with zero mean and variance of σ^2, i.e., $z_{\rm D} \sim C\mathcal{N}(0, \sigma^2)$.

Using (6), (7) and (9), we rewrite (11) as

$$y_{\rm D} = h_{\rm RD}\sqrt{P_{\rm R}}G(h_{\rm SR}\sqrt{P_{\rm S}}x_{\rm S} + I_{\rm R} + z_{\rm R}) + z_{\rm D}. \tag{12}$$

From (12), the end-to-end signal-to-interference-plus-noise ratios (SINRs) for the case of fixed gain (denoted by $\gamma_{\rm f}$) and variable gain (denoted by $\gamma_{\rm v}$) of the considered EH-FD-V2V relay system are respectively computed as

$$\gamma_{\rm f} = \frac{|h_{\rm SR}|^2|h_{\rm RD}|^2 P_{\rm S}P_{\rm R}}{|h_{\rm RD}|^2 P_{\rm R}(\gamma_{\rm RSI}+\sigma^2) + \sigma^2/G_{\rm f}^2} = \frac{|h_{\rm SR}|^4|h_{\rm RD}|^2\eta\alpha P_{\rm S}^2}{|h_{\rm SR}|^2|h_{\rm RD}|^2\eta\alpha P_{\rm S}(\gamma_{\rm RSI}+\sigma^2) + \sigma^2(1-\alpha)/G_{\rm f}^2}, \tag{13}$$

$$\gamma_{\rm v} = \frac{|h_{\rm SR}|^4|h_{\rm RD}|^2\eta\alpha P_{\rm S}^2}{|h_{\rm SR}|^2|h_{\rm RD}|^2\eta\alpha P_{\rm S}(\gamma_{\rm RSI}+\sigma^2) + \sigma^2(1-\alpha)(|h_{\rm SR}|^2 P_{\rm S} + \gamma_{\rm RSI}+\sigma^2)}. \tag{14}$$

3. System Performance

3.1. Outage Probability

The outage probability (OP) of the considered EH-FD-V2V relay system is defined as the probability that the instantaneous data transmission rate falls below a threshold [42]. Denote $\mathcal{R}$ (bit/s/Hz) as this threshold, then the OP of the considered EH-FD-V2V relay system is computed as

$$\mathcal{P}_{\text{out}} = \Pr\{(1-\alpha)\log_2(1+\gamma) < \mathcal{R}\} = \Pr\{\gamma < 2^{\frac{\mathcal{R}}{1-\alpha}} - 1\} = \Pr\{\gamma < \gamma_{\text{th}}\}, \tag{15}$$

where γ is end-to-end SINR given by in (13) and (14) for the cases of fixed and variable gains, respectively; $\gamma_{\text{th}} = 2^{\frac{\mathcal{R}}{1-\alpha}} - 1$ is the SINR threshold.

Based on (15), the OPs of the considered EH-FD-V2V relay system with fixed and variable gains under the impact of the cascade Rayleigh fading channels and RSI are provided in the following Theorem 1.

Theorem 1: Under the impact of RSI and cascade Rayleigh fading, the OPs in the case of fixed gain (denoted by $\mathcal{P}_{\text{out}_\text{f}}$) and variable gain (denoted by $\mathcal{P}_{\text{out}_\text{v}}$) of the considered EH-FD-V2V relay system are given by

$$\mathcal{P}_{\text{out}_\text{f}} = 1 - \frac{\pi}{2M}\exp(-A\gamma_{\text{th}})\sum_{m=1}^{M}\sqrt{1-\phi_m^2}\sqrt{\frac{B\gamma_{\text{th}}}{P_\text{S}G_\text{f}^2\Big(\ln\frac{1}{u} + A\gamma_{\text{th}}\Big)\ln\frac{1}{u}}} \times K_1\left(\sqrt{\frac{B\gamma_{\text{th}}}{P_\text{S}G_\text{f}^2\Big(\ln\frac{1}{u} + A\gamma_{\text{th}}\Big)\ln\frac{1}{u}}}\right), \tag{16}$$

$$\mathcal{P}_{\text{out}_\text{v}} = 1 - \frac{\pi}{2M}\exp(-A\gamma_{\text{th}})\sum_{m=1}^{M}\sqrt{1-\phi_m^2}\sqrt{\frac{B\Big[A(\gamma_{\text{th}}^2+\gamma_{\text{th}}) + \gamma_{\text{th}}\ln\frac{1}{u}\Big]}{\Big(\ln\frac{1}{u} + A\gamma_{\text{th}}\Big)\ln\frac{1}{u}}} \times K_1\left(\sqrt{\frac{B\Big[A(\gamma_{\text{th}}^2+\gamma_{\text{th}}) + \gamma_{\text{th}}\ln\frac{1}{u}\Big]}{\Big(\ln\frac{1}{u} + A\gamma_{\text{th}}\Big)\ln\frac{1}{u}}}\right), \tag{17}$$

where $A = \frac{\gamma_{\text{RSI}}+\sigma^2}{P_\text{S}}; B = \frac{4\sigma^2(1-\alpha)}{\eta\alpha P_\text{S}}$; M is the complexity-accuracy trade-off parameter; $\phi_m = \cos\Big(\frac{(2m-1)\pi}{2M}\Big)$; $u = \frac{1}{2}(\phi_m + 1)$; $K_1(.)$ denotes the first order modified Bessel function of the second kind [43].

Proof: The detailed proofs are presented in Appendix A.

3.2. Symbol Error Probability

The SEP of the considered EH-FD-V2V relay system can be calculated as [42]

$$\text{SEP} = a\mathbb{E}\{Q(\sqrt{b\gamma})\} = \frac{a}{\sqrt{2\pi}}\int_0^\infty F\Big(\frac{t^2}{b}\Big)\exp\Big(-\frac{t^2}{2}\Big)dt, \tag{18}$$

where $Q(x) = \frac{1}{\sqrt{2\pi}}\int\limits_x^\infty e^{-t^2/2}dt$ is the Gaussian function; (a, b) are constants and their values are determined by the modulation types [42]. For examples, $(a, b) = (1, 2)$ for the binary phase-shift keying (BPSK) and $(a, b) = (2, 1)$ for the 4-quadrature amplitude modulation (4-QAM); γ and $F(.)$ are respectively the end-to-end SINR and its CDF.

After some basic algebra calculations, (18) becomes

$$\text{SEP} = \frac{a\sqrt{b}}{2\sqrt{2\pi}}\int_0^\infty \frac{\exp(-bx/2)}{\sqrt{x}}F(x)dx. \tag{19}$$

Based on (19), the SEPs of the considered EH-FD-V2V relay system with fixed and variable gains are given in the following Theorem 2.

Theorem 2: The SEPs of the considered EH-FD-V2V relay system in the case of fixed gain (denoted by $\mathrm{SEP_f}$) and variable gain (denoted by $\mathrm{SEP_v}$) are computed as

$$\mathrm{SEP_f} = \frac{a\sqrt{b}}{2\sqrt{2\pi}}\left[\sqrt{\frac{2\pi}{b}} - \frac{\pi^2}{4MN(A+b/2)}\sum_{m=1}^{M}\sum_{n=1}^{N}\sqrt{(1-\phi_m^2)(1-\phi_n^2)}\sqrt{\frac{B}{P_S G_f^2\left(\frac{A\ln\frac{1}{v}}{A+b/2}+\ln\frac{1}{u}\right)\ln\frac{1}{u}}}\right.$$
$$\left.\times K_1\left(\sqrt{\frac{B\ln\frac{1}{v}}{P_S G_f^2(A+b/2)\left(\frac{A\ln\frac{1}{v}}{A+b/2}+\ln\frac{1}{u}\right)\ln\frac{1}{u}}}\right)\right], \tag{20}$$

$$\mathrm{SEP_v} = \frac{a\sqrt{b}}{2\sqrt{2\pi}}\left[\sqrt{\frac{2\pi}{b}} - \frac{\pi^2}{4MN(A+b/2)}\sum_{m=1}^{M}\sum_{n=1}^{N}\sqrt{(1-\phi_m^2)(1-\phi_n^2)}\sqrt{\frac{B\left[\frac{A\ln\frac{1}{v}}{A+b/2}+\ln\frac{1}{u}+A\right]}{\left(\frac{A\ln\frac{1}{v}}{A+b/2}+\ln\frac{1}{u}\right)\ln\frac{1}{u}}}\right.$$
$$\left.\times K_1\left(\sqrt{\frac{B\left[A\left(\frac{\ln\frac{1}{v}}{A+b/2}\right)^2+\frac{A\ln\frac{1}{v}}{A+b/2}+\frac{\ln\frac{1}{v}\ln\frac{1}{u}}{A+b/2}\right]}{\left(\frac{A\ln\frac{1}{v}}{A+b/2}+\ln\frac{1}{u}\right)\ln\frac{1}{u}}}\right)\right], \tag{21}$$

where N is the complexity-accuracy trade-off parameter; $\phi_n = \cos\left(\frac{(2n-1)\pi}{2N}\right)$; $v = \frac{1}{2}(\phi_n + 1)$.

Proof: The detailed proofs are presented in Appendix B.

4. Numerical Results and Discussion

Using the exact closed-form expressions of the OP and SEP in the previous section, we exhaustively investigate the performance of the considered EH-FD-V2V relay system through various evaluating scenarios. In the following figures, the curves represent the analysis results while the markers refer to Monte-Carlo simulation results. To further show the impact of cascade Rayleigh fading on the performance of the considered EH-FD-V2V relay system, we also provide the OP and SEP of the system for both fixed and variable gains over Rayleigh fading (denoted by "Ray-fa" on the figures). Moreover, we define the average SNR as the ratio of the average transmission power of S to the variance of AWGN, i.e., SNR $= P_S/\sigma^2$. Otherwise stated, the time switching ratio $\alpha = 0.5$, the energy harvesting efficiency $\eta = 0.85$, and the SIC capability $k = -30$ dB.

Fig. 2 illustrates the OP of the considered EH-FD-V2V relay system versus the average SNR in comparison with the OP of this system over the Rayleigh fading channel. We choose the data transmission rate $\mathcal{R} = 0.3$ bit/s/Hz. The analysis results are plotted by using (16) and (17) in Theorem 1 for the cases of fixed and variable gains, respectively. Moreover, we also simulate the OPs of the considered EH-FD-V2V relay system for both fixed and variable gains with nonlinear energy harvester when the saturation power threshold is $P_{\mathrm{th}}/\sigma^2 = 25$ dB to compare with the OPs of this system with linear energy harvester. It is obvious that the OP of the considered EH-FD-V2V relay system over cascade Rayleigh fading is significantly reduced in comparison with the OP of that system over Rayleigh fading. Specifically, to obtain OP $= 10^{-2}$, the SNR of the system over cascade Rayleigh fading need to be 4 dB and 5 dB higher for the case of fixed and variable gains, respectively. The similar behavior can be observed in [44–46]. In addition, due to the effect of saturation power threshold, the OPs with nonlinear energy harvester go to the floor faster, especially for the case of fixed gain relaying. Furthermore, the OP performance with variable gain is much better than that with fixed gain. The SNR benefit with variable gain compared with fixed gain is

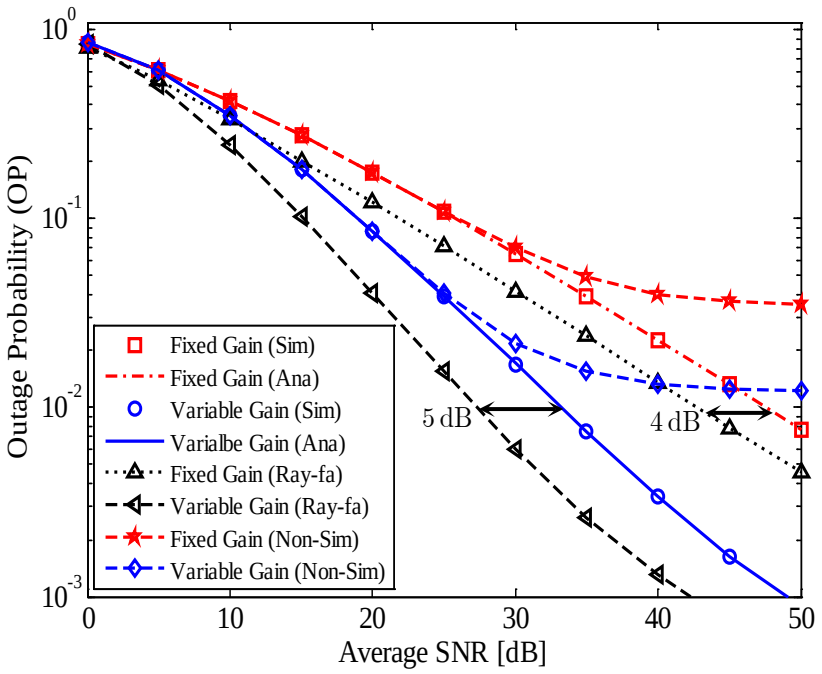

Figure 2: The OP of the considered EH-FD-V2V relay system vs. the average SNR in comparison with the OP of this system over Rayleigh fading channels, $\mathcal{R} = 0.3$ bit/s/Hz.

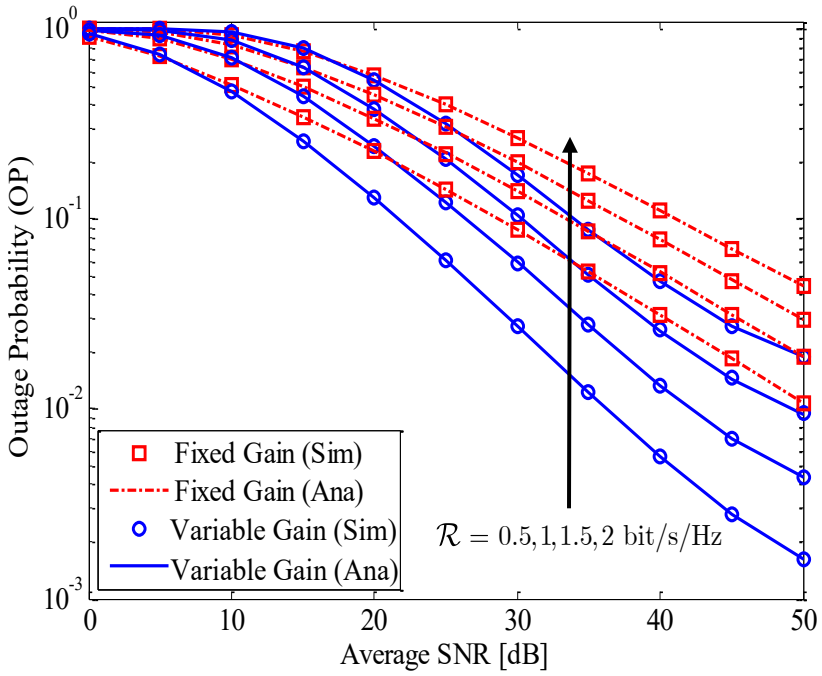

Figure 3: The OP of the considered EH-FD-V2V relay system vs. the average SNR for various data transmission rates.

about 20 dB at OP $= 10^{-2}$. Therefore, it is important to use variable gain instead of fixed gain for the considered EH-FD-V2V relay system to achieve lower OP.

Fig. 3 shows the impact of the data transmission rate on the OP of the considered EH-FD-V2V relay system. The data transmission rate is varied as $\mathcal{R} = 0.5, 1, 1.5, 2$ bit/s/Hz. We can see in Fig. 3 that, for the low data

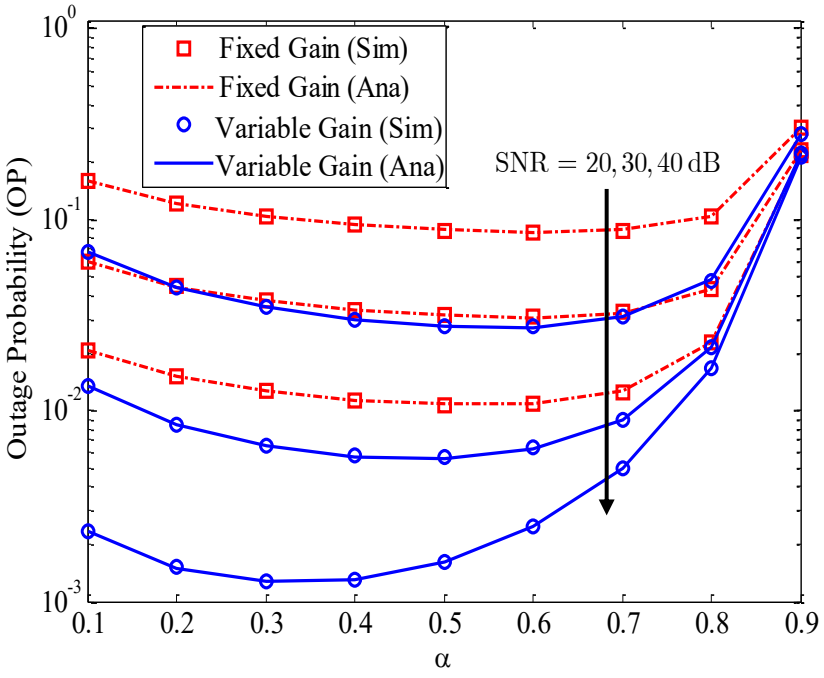

Figure 4: The impact of time switching ratio α on the OP of the considered EH-FD-V2V relay system for different values of SNR; $\mathcal{R} = 0.5$ bit/s/Hz.

transmission rate, i.e., $\mathcal{R} = 0.5$ bit/s/Hz, the OPs reach 10^{-2} and 2×10^{-3} at SNR = 50 dB for the cases of fixed and variable gains, respectively. However, for higher data transmission rate, especially when $\mathcal{R} = 2$ bit/s/Hz, the OPs only reach 8×10^{-2} and 3×10^{-2} at SNR = 50 dB for the cases of fixed and variable gains, respectively. It is because this system uses a half time duration ($\alpha = 0.5$) for EH, thus the time duration for the data transmission is only a half, which greatly reduces the OP performance of the considered EH-FD-V2V relay system. Therefore, to maintain the OP performance, a low data transmission rate should be used. Additionally, the time switching ratio α has a strong effect on the OP. Thus, in the next figure, we will evaluate the impact of α on the OPs for both cases of fixed and variable gains.

Fig. 4 depicts the impact of time switching ratio α on the OP of the considered EH-FD-V2V relay system for different values of SNR. We use (16) and (17) to plot analysis curves. It is noted that the terms A and B in these expressions are functions of α when setting the SNR and other parameter as constants. Therefore, the OPs with fixed and variable gain relaying are also functions of time switching ratio α. We can see that for a certain SNR there are optimal values of α that minimize the OP of fixed and variable gains. For examples, when SNR = 20 dB, the optimal values are $\alpha = 0.6$ and $\alpha = 0.5$ for fixed and variable gains, respectively. As the SNR increases, these values are reduced, e.g., when SNR = 40 dB, the optimal values are $\alpha = 0.5$ and $\alpha = 0.3$ for fixed and variable gains, respectively. These results are suitable for the considered system because when the SNR is low, R needs more time for EH. Therefore, the time duration for data transmission is reduced. However, when the SNR is high, R can harvest enough energy in a short time, leading to a decrease in the time duration for EH. As a result, based on the average transmission power of S and the type of gain relaying used at R, we can choose a suitable the EH time duration for R to significantly improve the OP performance of the considered EH-FD-V2V relay system.

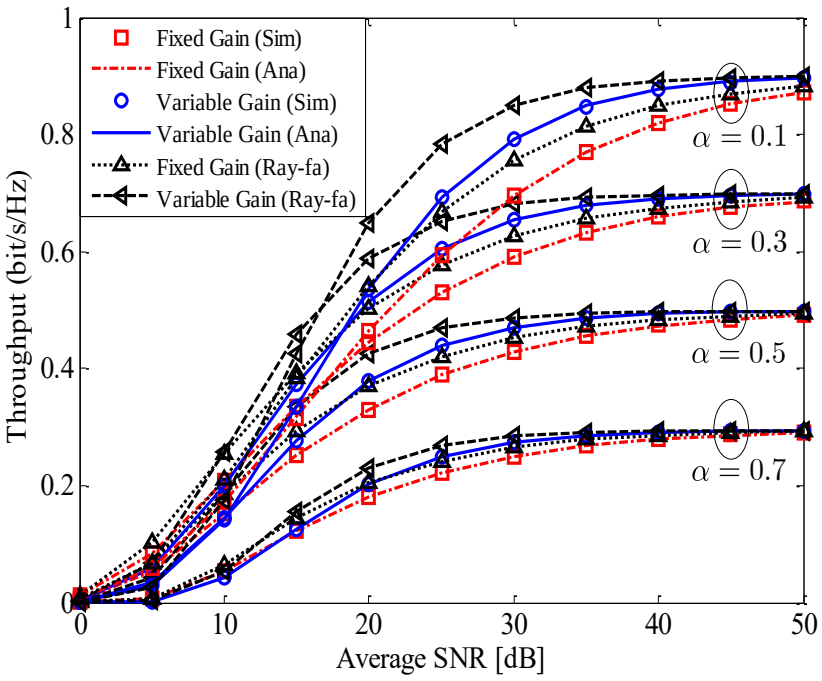

Figure 5: The throughput of the considered EH-FD-V2V relay system vs. the average SNR for different time switching ratio α; $\mathcal{R} = 1$ bit/s/Hz.

In Fig. 5, we investigate the throughput of the considered EH-FD-V2V relay system versus the average SNR for various time switching ratio α. This throughput is calculated as $\mathcal{T}_{\text{put}} = \mathcal{R}(1-\alpha)(1-\mathcal{P}_{\text{out}})$, where $\mathcal{P}_{\text{out}}$ are given in (16) and (17) for the cases of fixed and variable gains, respectively. As can be seen from Fig. 5, the lower value of α leads to a higher throughput. For example, when $\alpha = 0.1$, the throughput nearly reaches 0.9 bit/s/Hz at SNR = 50 dB for both cases of fixed and variable gains. However, for the higher α, especially when $\alpha = 0.7$, the throughput only reaches 0.3 bit/s/Hz at SNR = 50 dB for both cases of fixed and variable gains. It is also noted that lower α leads to higher throughput due to the higher time duration for data exchange. However, lower α will reduce the OP performance, especially in the low SNR region. Therefore, using both Fig. 4 and Fig. 5, we can choose a suitable α for the considered EH-FD-V2V relay system based on the requirements of the OP and throughput.

Fig. 6 plots the SEP of the considered EH-FD-V2V relay system with BPSK modulation ($a = 1, b = 2$) versus the average SNR for both fixed and variable gains. We also provide the SEP of this system over Rayleigh fading channels for both fixed and variable gains. The analysis curves in Fig. 6 are plotted by using (20) and (21) for fixed and variable gains, respectively. Similar to the OP, the SEP of the considered EH-FD-V2V relay system is higher than that of this system over Rayleigh fading. Furthermore, the SEP with variable gain is much lower than that with fixed gain, and the SEP of the considered EH-FD-V2V relay system will go to error floor in high SNR regime.

Fig. 7 presents the impact of the RSI on the SEP of the considered EH-FD-V2V relay system. As can be seen from Fig. 7, the RSI significantly affects the SEP, especially in the high SNR regime. Notably, in the low SNR regime (SNR $<$ 20 dB), SEPs of fixed and variable gains are nearly similar. However, in the high SNR regime, the difference between them is remarkable. Furthermore, since the RSI power increases with the transmission power

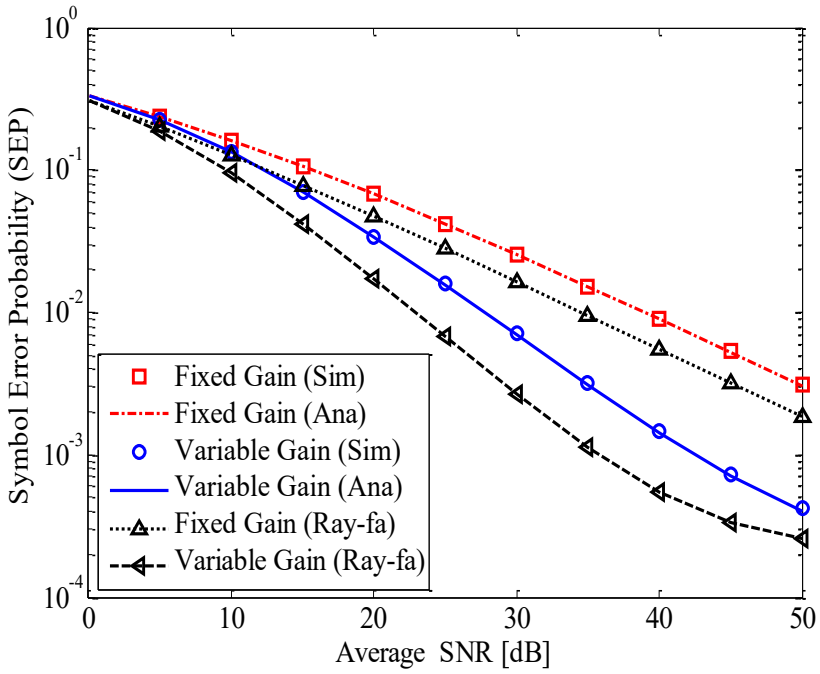

Figure 6: The SEP of the considered EH-FD-V2V relay system with BPSK modulation vs. the average SNR.

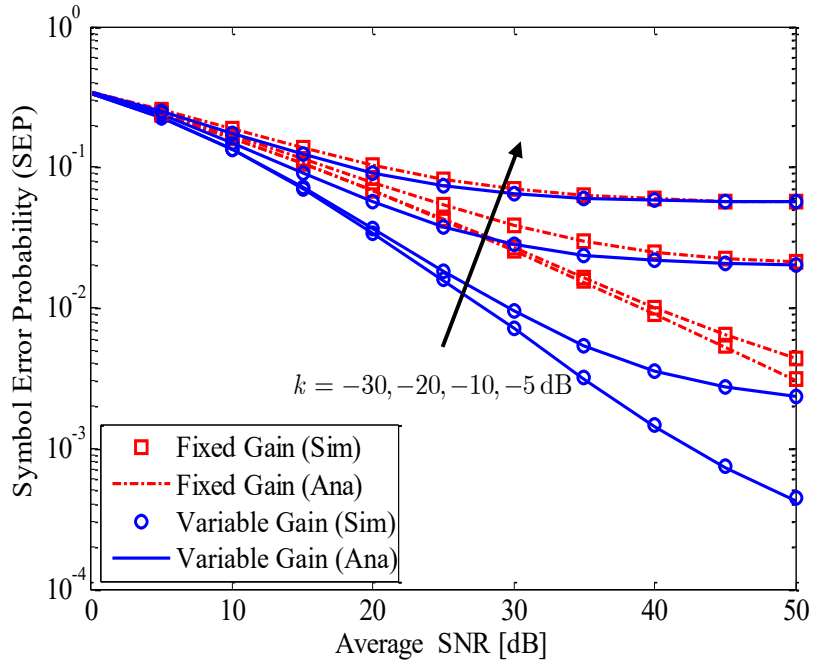

Figure 7: The impact of RSI on the SEP of the considered EH-FD-V2V relay system for different RSI levels.

of S (refers to (5)), high SNR leads to high RSI power. With low RSI level, i.e., $k = -30$ dB, SEPs for both fixed and variable gains still decrease in the evaluating SNR range. However, for higher RSI level, e.g., $k = -20$ dB, the SEPs of both cases fall slowly, especially for variable gain. In the case of $k = -10$ dB and $k = -5$ dB, the SEPs for both fixed and variable gains are similar. On the other hand, with the investigated RSI levels, SEPs decrease slowly and go to error floor earlier when SNR increases. When RSI level is small, SEP of variable gain is always

lower than that of fixed gain, especially in high SNR regime. However, when the RSI level is large enough, SEPs of both fixed and variable gains are similar in the high SNR regime. Therefore, more efforts are needed to improve the SIC capability of FD relay so that higher system performance can be achieved.

5. Conclusion

Realizing the advantages of combining both EH and FD in V2V communications, in this paper, we conducted a performance evaluation of EH-FD-V2V relay system under the impact of RSI due to FD transmission over cascade Rayleigh fading channels. We successfully obtained the exact expressions of the OP and SEP of the considered EH-FD-V2V relay system for both cases, i.e., fixed and variable gains at FD relay. Numerical results showed that the performance of this system is significantly reduced due to the cascade Rayleigh fading. Additionally, the performance of the considered system with variable gain is considerably better than that with fixed gain. We also observed that, with a specific transmission power of the source, there is an optimal time switching ratio that minimizes the OP of the considered EH-FD-V2V relay system. However, the optimal time switching ratio with fixed gain is different from that with variable gain. Therefore, depending on the transmission power of source and the type of gain relaying used at FD relay, we can choose a suitable time switching ratio to achieve the best system performance. On the other hand, reducing the RSI is also crucial in the considered EH-FD-V2V relay system.

Appendix A

This appendix provides the detailed derivations of the OP expressions in Theorem 1.

For the case of variable gain, we calculate the OP by replacing $\gamma_{\rm v}$ in (14) into (15), i.e.,

$$\mathcal{P}_{\rm out_v} = \Pr\left\{\frac{|h_{\rm SR}|^4|h_{\rm RD}|^2\eta\alpha P_{\rm S}^2}{|h_{\rm SR}|^2|h_{\rm RD}|^2\eta\alpha P_{\rm S}(\gamma_{\rm RSI}+\sigma^2)+\sigma^2(1-\alpha)(|h_{\rm SR}|^2P_{\rm S}+\gamma_{\rm RSI}+\sigma^2)} < \gamma_{\rm th}\right\}. \tag{22}$$

To solve the probability in (22), we consider the Rayleigh fading channel first. The cumulative distribution function (CDF, denoted by $F(.)$), and the probability density function (PDF, denoted by $f(.)$) of the instantaneous channel gain $|h_{\rm SR}|^2$ of Rayleigh fading channel are given by

$$F_{|h_{\rm SR}|^2}(x) = 1-\exp\Big(-\frac{x}{\Omega}\Big), x \geqslant 0, \tag{23}$$

$$f_{|h_{\rm SR}|^2}(x) = \frac{1}{\Omega}\exp\Big(-\frac{x}{\Omega}\Big), x \geqslant 0. \tag{24}$$

where $\Omega = \mathbb{E}\{|h|^2\}$ is the average channel gain.

In this paper, we normalize all the average channel gains, i.e., $\Omega = 1$. Therefore, (23) and (24) become

$$F_{|h_{\rm SR}|^2}(x) = 1-\exp(-x), x \geqslant 0, \tag{25}$$

$$f_{|h_{\rm SR}|^2}(x) = \exp(-x), x \geqslant 0. \tag{26}$$

On the other hand, the R – D channel is cascade Rayleigh fading channel. Therefore, the CDF and PDF of $|h_{\rm RD}|^2$ are respectively calculated as [17, 19, 31]

$$F_{|h_{\rm RD}|^2}(x) = 1 - \sqrt{4x}K_1\Big(\sqrt{4x}\Big), \tag{27}$$

$$f_{|h_{\rm RD}|^2}(x) = 2K_0\Big(\sqrt{4x}\Big), \tag{28}$$

where $K_0(.)$ is the zero-order modified Bessel function of the second kind [43].

Based on the CDF and PDF of $|h_{\rm SR}|^2$ and $|h_{\rm RD}|^2$, we can now calculate the OP of the considered EH-FD-V2V relay system from (22) as follows

$$\begin{aligned}\mathcal{P}_{\rm out_v} &= \Pr\left\{\frac{|h_{\rm SR}|^4|h_{\rm RD}|^2\eta\alpha P_{\rm S}^2}{|h_{\rm SR}|^2|h_{\rm RD}|^2\eta\alpha P_{\rm S}(\gamma_{\rm RSI}+\sigma^2)+\sigma^2(1-\alpha)(|h_{\rm SR}|^2P_{\rm S}+\gamma_{\rm RSI}+\sigma^2)} < \gamma_{\rm th}\right\}\\ &= \Pr\left\{|h_{\rm SR}|^2|h_{\rm RD}|^2\eta\alpha P_{\rm S}\Big[|h_{\rm SR}|^2P_{\rm S}-\gamma_{\rm th}(\gamma_{\rm RSI}+\sigma^2)\Big] < \gamma_{\rm th}\sigma^2(1-\alpha)(|h_{\rm SR}|^2P_{\rm S}+\gamma_{\rm RSI}+\sigma^2)\right\}.\end{aligned} \tag{29}$$

Let $|h_{\rm SR}|^2 = y + \frac{\gamma_{\rm th}(\gamma_{\rm RSI}+\sigma^2)}{P_{\rm S}}$, we rewrite (29) as

$$\begin{aligned}\mathcal{P}_{\rm out_v} &= \Pr\left\{|h_{\rm RD}|^2 < \frac{\sigma^2(1-\alpha)\Big[(\gamma_{\rm RSI}+\sigma^2)(\gamma_{\rm th}^2+\gamma_{\rm th})+P_{\rm S}y\gamma_{\rm th}\Big]}{\eta\alpha P_{\rm S}y\Big[P_{\rm S}y+(\gamma_{\rm RSI}+\sigma^2)\gamma_{\rm th}\Big]}\right\}\\ &= 1-\int_0^\infty\left[1-F_{|h_{\rm RD}|^2}\left(\frac{\sigma^2(1-\alpha)\Big[(\gamma_{\rm RSI}+\sigma^2)(\gamma_{\rm th}^2+\gamma_{\rm th})+P_{\rm S}y\gamma_{\rm th}\Big]}{\eta\alpha P_{\rm S}y\Big[P_{\rm S}y+(\gamma_{\rm RSI}+\sigma^2)\gamma_{\rm th}\Big]}\right)\right]\times f_{|h_{\rm SR}|^2}\Big(y+\frac{\gamma_{\rm th}(\gamma_{\rm RSI}+\sigma^2)}{P_{\rm S}}\Big)dy.\end{aligned} \tag{30}$$

Using (27) and (26), (30) becomes

$$\begin{aligned}\mathcal{P}_{\rm out_v} = 1-&\int_0^\infty\sqrt{\frac{4\sigma^2(1-\alpha)\Big[(\gamma_{\rm RSI}+\sigma^2)(\gamma_{\rm th}^2+\gamma_{\rm th})+P_{\rm S}y\gamma_{\rm th}\Big]}{\eta\alpha P_{\rm S}y\Big[P_{\rm S}y+(\gamma_{\rm RSI}+\sigma^2)\gamma_{\rm th}\Big]}}\\ &\times K_1\left(\sqrt{\frac{4\sigma^2(1-\alpha)\Big[(\gamma_{\rm RSI}+\sigma^2)(\gamma_{\rm th}^2+\gamma_{\rm th})+P_{\rm S}y\gamma_{\rm th}\Big]}{\eta\alpha P_{\rm S}y\Big[P_{\rm S}y+(\gamma_{\rm RSI}+\sigma^2)\gamma_{\rm th}\Big]}}\right)\exp\Big(-y-\frac{\gamma_{\rm th}(\gamma_{\rm RSI}+\sigma^2)}{P_{\rm S}}\Big)dy.\end{aligned} \tag{31}$$

By setting $z = \exp(-y)$, (31) can be rewritten as

$$\begin{aligned}\mathcal{P}_{\rm out_v} =&1-\exp\Big(-\frac{\gamma_{\rm th}(\gamma_{\rm RSI}+\sigma^2)}{P_{\rm S}}\Big)\int_0^1\sqrt{\frac{4\sigma^2(1-\alpha)\Big[(\gamma_{\rm RSI}+\sigma^2)(\gamma_{\rm th}^2+\gamma_{\rm th})+P_{\rm S}\gamma_{\rm th}\ln\frac{1}{z}\Big]}{\eta\alpha P_{\rm S}\Big[P_{\rm S}\ln\frac{1}{z}+(\gamma_{\rm RSI}+\sigma^2)\gamma_{\rm th}\Big]\ln\frac{1}{z}}}\\ &\times K_1\left(\sqrt{\frac{4\sigma^2(1-\alpha)\Big[(\gamma_{\rm RSI}+\sigma^2)(\gamma_{\rm th}^2+\gamma_{\rm th})+P_{\rm S}\gamma_{\rm th}\ln\frac{1}{z}\Big]}{\eta\alpha P_{\rm S}\Big[P_{\rm S}\ln\frac{1}{z}+(\gamma_{\rm RSI}+\sigma^2)\gamma_{\rm th}\Big]\ln\frac{1}{z}}}\right)dz\\ =&1-\exp(-A\gamma_{\rm th})\int_0^1\sqrt{\frac{B\Big[A(\gamma_{\rm th}^2+\gamma_{\rm th})+\gamma_{\rm th}\ln\frac{1}{z}\Big]}{\Big(\ln\frac{1}{z}+A\gamma_{\rm th}\Big)\ln\frac{1}{z}}}K_1\left(\sqrt{\frac{B\Big[A(\gamma_{\rm th}^2+\gamma_{\rm th})+\gamma_{\rm th}\ln\frac{1}{z}\Big]}{\Big(\ln\frac{1}{z}+A\gamma_{\rm th}\Big)\ln\frac{1}{z}}}\right)dz.\end{aligned} \tag{32}$$

Applying the Gaussian-Chebyshev quadrature method [47] for the integral in (32), we have

$$\int_0^1 \sqrt{\frac{B\Big[A(\gamma_{\rm th}^2+\gamma_{\rm th})+\gamma_{\rm th}\ln\frac{1}{z}\Big]}{\Big(\ln\frac{1}{z}+A\gamma_{\rm th}\Big)\ln\frac{1}{z}}}K_1\left(\sqrt{\frac{B\Big[A(\gamma_{\rm th}^2+\gamma_{\rm th})+\gamma_{\rm th}\ln\frac{1}{z}\Big]}{\Big(\ln\frac{1}{z}+A\gamma_{\rm th}\Big)\ln\frac{1}{z}}}\right)dz$$
$$=\frac{\pi}{2M}\sum_{m=1}^{M}\sqrt{1-\phi_m^2}\sqrt{\frac{B\Big[A(\gamma_{\rm th}^2+\gamma_{\rm th})+\gamma_{\rm th}\ln\frac{1}{u}\Big]}{\Big(\ln\frac{1}{u}+A\gamma_{\rm th}\Big)\ln\frac{1}{u}}}K_1\left(\sqrt{\frac{B\Big[A(\gamma_{\rm th}^2+\gamma_{\rm th})+\gamma_{\rm th}\ln\frac{1}{u}\Big]}{\Big(\ln\frac{1}{u}+A\gamma_{\rm th}\Big)\ln\frac{1}{u}}}\right), \tag{33}$$

where M, ϕ_m, and u are defined in Theorem 1.

Substituting (33) into (32), we obtain the OP of the considered EH-FD-V2V relay system in the case of variable gain as in (17) of Theorem 1.

Similarly, by doing all mathematical derivation steps above for the OP in the case of fixed gain, we obtain (16). The proof is complete.

Appendix B

This appendix provides the detailed derivations of the SEP expressions in Theorem 2.

To calculate SEP from (19), we firstly need to obtain the CDF, $F(x)$, of the end-to-end SINR from its definition, i.e.,

$$F(x)=\Pr\{\gamma<x\}, \tag{34}$$

where γ is the end-to-end SINR.

Meanwhile, the OP is calculated from (15). Therefore, we can replace $\gamma_{\rm th}$ in (16) and (17) by x to obtain the $F(x)$ for the cases of fixed gain and variable gain, respectively. For the case of variable gain, $F(x)$ is given by

$$F(x)=1-\frac{\pi}{2M}\exp(-Ax)\sum_{m=1}^{M}\sqrt{1-\phi_m^2}\sqrt{\frac{B\Big[A(x^2+x)+x\ln\frac{1}{u}\Big]}{\Big(\ln\frac{1}{u}+Ax\Big)\ln\frac{1}{u}}}K_1\left(\sqrt{\frac{B\Big[A(x^2+x)+x\ln\frac{1}{u}\Big]}{\Big(\ln\frac{1}{u}+Ax\Big)\ln\frac{1}{u}}}\right). \tag{35}$$

Replacing $F(x)$ in (35) into (19), we can compute $\mathrm{SEP_v}$ as

$$\mathrm{SEP_v}=\frac{a\sqrt{b}}{2\sqrt{2\pi}}\Bigg[\int_0^\infty\frac{\exp(-bx/2)}{\sqrt{x}}dx-\frac{\pi}{2M}\sum_{m=1}^{M}\sqrt{1-\phi_m^2}\int_0^\infty\exp\Big(-(A+b/2)x\Big)\sqrt{\frac{B\Big[Ax+\ln\frac{1}{u}+A\Big]}{\Big(Ax+\ln\frac{1}{u}\Big)\ln\frac{1}{u}}}$$
$$\times K_1\left(\sqrt{\frac{B\Big[Ax^2+Ax+x\ln\frac{1}{u}\Big]}{\Big(Ax+\ln\frac{1}{u}\Big)\ln\frac{1}{u}}}\right)dx\Bigg]. \tag{36}$$

Using [43, Eq. (3.361.2)] for the first integral in (36), we have

$$\int_0^\infty\frac{\exp(-bx/2)}{\sqrt{x}}dx=\sqrt{\frac{2\pi}{b}}. \tag{37}$$

To solve the second integral in (36), we use a change of variables, i.e., $t = \exp\Big(-(A+b/2)x\Big)$. After some mathematical transforms, we have

$$\int_0^{\infty} \exp\Big(-(A+b/2)x\Big)\sqrt{\frac{B\Big[Ax+\ln\frac{1}{u}+A\Big]}{\Big(Ax+\ln\frac{1}{u}\Big)\ln\frac{1}{u}}}K_1\Bigg(\sqrt{\frac{B\Big[Ax^2+Ax+x\ln\frac{1}{u}\Big]}{\Big(Ax+\ln\frac{1}{u}\Big)\ln\frac{1}{u}}}\Bigg)dx$$
$$= \frac{1}{A+b/2}\int_0^{1}\sqrt{\frac{B\Big[\frac{A\ln\frac{1}{t}}{A+b/2}+\ln\frac{1}{u}+A\Big]}{\Big(\frac{A\ln\frac{1}{t}}{A+b/2}+\ln\frac{1}{u}\Big)\ln\frac{1}{u}}}K_1\Bigg(\sqrt{\frac{B\Big[A\Big(\frac{\ln\frac{1}{t}}{A+b/2}\Big)^2+\frac{A\ln\frac{1}{t}}{A+b/2}+\frac{\ln\frac{1}{t}\ln\frac{1}{u}}{A+b/2}\Big]}{\Big(\frac{A\ln\frac{1}{t}}{A+b/2}+\ln\frac{1}{u}\Big)\ln\frac{1}{u}}}\Bigg)dt \tag{38}$$

Applying the Gaussian-Chebyshev quadrature method [47], the integral in (38) is calculated as

$$\frac{1}{A+b/2}\int_0^{1}\sqrt{\frac{B\Big[\frac{A\ln\frac{1}{t}}{A+b/2}+\ln\frac{1}{u}+A\Big]}{\Big(\frac{A\ln\frac{1}{t}}{A+b/2}+\ln\frac{1}{u}\Big)\ln\frac{1}{u}}}K_1\Bigg(\sqrt{\frac{B\Big[A\Big(\frac{\ln\frac{1}{t}}{A+b/2}\Big)^2+\frac{A\ln\frac{1}{t}}{A+b/2}+\frac{\ln\frac{1}{t}\ln\frac{1}{u}}{A+b/2}\Big]}{\Big(\frac{A\ln\frac{1}{t}}{A+b/2}+\ln\frac{1}{u}\Big)\ln\frac{1}{u}}}\Bigg)dt$$
$$= \frac{\pi}{2N(A+b/2)}\sum_{n=1}^{N}\sqrt{1-\phi_n^2}\sqrt{\frac{B\Big[\frac{A\ln\frac{1}{v}}{A+b/2}+\ln\frac{1}{u}+A\Big]}{\Big(\frac{A\ln\frac{1}{v}}{A+b/2}+\ln\frac{1}{u}\Big)\ln\frac{1}{u}}}K_1\Bigg(\sqrt{\frac{B\Big[A\Big(\frac{\ln\frac{1}{v}}{A+b/2}\Big)^2+\frac{A\ln\frac{1}{v}}{A+b/2}+\frac{\ln\frac{1}{v}\ln\frac{1}{u}}{A+b/2}\Big]}{\Big(\frac{A\ln\frac{1}{v}}{A+b/2}+\ln\frac{1}{u}\Big)\ln\frac{1}{u}}}\Bigg), \tag{39}$$

where N, ϕ_n, and v are defined in Theorem 2.

Substituting (37), (38), and (39) into (36), we obtain the exact closed-form expression of the SEP of the considered EH-FD-V2V relay system in the case of variable gain as in (21). The SEP in the case of fixed gain can be obtained by similar ways. The proof is complete.

References

[1] Y. Deng, K. J. Kim, T. Q. Duong, M. Elkashlan, G. K. Karagiannidis, A. Nallanathan, Full-duplex spectrum sharing in cooperative single carrier systems, IEEE Transactions on Cognitive Communications and Networking 2 (1) (2016) 68–82.

[2] X.-T. Doan, N.-P. Nguyen, C. Yin, D. B. Da Costa, T. Q. Duong, Cognitive full-duplex relay networks under the peak interference power constraint of multiple primary users, EURASIP Journal on Wireless Communications and Networking 2017 (1) (2017) 8.

[3] A. H. Gazestani, S. A. Ghorashi, B. Mousavinasab, M. Shikh-Bahaei, A survey on implementation and applications of full duplex wireless communications, Physical Communication 34 (2019) 121–134.

[4] M. Imran, L. U. Khan, I. Yaqoob, E. Ahmed, M. A. Qureshi, A. Ahmed, Energy harvesting in 5G networks: Taxonomy, requirements, challenges, and future directions, arXiv preprint arXiv:1910.00785.

[5] B. C. Nguyen, X. N. Tran, D. T. Tran, Performance analysis of in-band full-duplex amplify-and-forward relay system with direct link, in: Recent Advances in Signal Processing, Telecommunications & Computing (SigTelCom), 2018 2nd International Conference on, IEEE, 2018, pp. 192–197.

[6] O. Abbasi, A. Ebrahimi, Cooperative NOMA with full-duplex amplify-and-forward relaying, Transactions on Emerging Telecommunications Technologies 29 (7) (2018) e3421.

[7] G. Chen, J. P. Coon, A. Mondal, B. Allen, J. A. Chambers, Performance analysis for multihop full-duplex IoT networks subject to poisson distributed interferers, IEEE Internet of Things Journal 6 (2) (2018) 3467–3479.

[8] R. Rezaei, S. Sun, X. Kang, Y. L. Guan, M. R. Pakravan, Secrecy throughput maximization for full-duplex wireless powered IoT networks under fairness constraints, IEEE Internet of Things Journal.

[9] L. V. Nguyen, B. C. Nguyen, X. N. Tran, L. T. Dung, Closed-form expression for the symbol error probability in full-duplex spatial modulation relay system and its application in optimal power allocation, Sensors 19 (24) (2019) 5390.

[10] K. E. Kolodziej, B. T. Perry, J. S. Herd, In-band full-duplex technology: Techniques and systems survey, IEEE Transactions on Microwave Theory and Techniques.

[11] B. C. Nguyen, X. N. Tran, Performance analysis of full-duplex amplify-and-forward relay system with hardware impairments and imperfect self-interference cancellation, Wireless Communications and Mobile Computing 2019 (2019) 10. doi:10.1155/2019/4946298.

[12] J. Wang, H. Yu, Y. Wu, F. Shu, J. Wang, R. Chen, J. Li, Pilot optimization and power allocation for OFDM-based full-duplex relay networks with IQ-imbalances, IEEE Access 5 (2017) 24344–24352.

[13] F. Shu, Y. Zhou, R. Chen, J. Wang, J. Li, B. Vucetic, High-performance beamformer and low-complexity detector for DF-based full-duplex MIMO relaying networks, China Communications 14 (2) (2017) 173–182.

[14] H. H. M. Tam, H. D. Tuan, A. A. Nasir, T. Q. Duong, H. V. Poor, MIMO energy harvesting in full-duplex multi-user networks, IEEE Transactions on Wireless Communications 16 (5) (2017) 3282–3297.

[15] D. Bharadia, E. McMilin, S. Katti, Full duplex radios, in: ACM SIGCOMM Computer Communication Review, Vol. 43, ACM, 2013, pp. 375–386.

[16] C. Li, Z. Chen, Y. Wang, Y. Yao, B. Xia, Outage analysis of the full-duplex decode-and-forward two-way relay system, IEEE Trans. Veh. Technol. 66 (5) (2017) 4073–4086. doi:10.1109/TVT.2016.2610004.

[17] B. C. Nguyen, X. N. Tran, T. M. Hoang, L. T. Dung, Performance analysis of full-duplex vehicle-to-vehicle relay system over double-rayleigh fading channels, Mobile Networks and Applications (2019) 1–10.

[18] C. Campolo, A. Molinaro, A. O. Berthet, A. Vinel, Full-duplex radios for vehicular communications, IEEE Communications Magazine 55 (6) (2017) 182–189.

[19] B. C. Nguyen, T. M. Hoang, L. T. Dung, Performance analysis of vehicle-to-vehicle communication with full-duplex amplify-and-forward relay over double-rayleigh fading channels, Vehicular Communications 19 (2019) 100166.

[20] C.-X. Mao, S. Gao, Y. Wang, Dual-band full-duplex Tx/Rx antennas for vehicular communications, IEEE Transactions on Vehicular Technology 67 (5) (2018) 4059–4070.

[21] M. Yang, S.-W. Jeon, D. K. Kim, Interference management for in-band full-duplex vehicular access networks, IEEE Transactions on Vehicular Technology 67 (2) (2018) 1820–1824.

[22] B. C. Nguyen, T. M. Hoang, P. T. Tran, T. N. Nguyen, Outage probability of noma system with wireless power transfer at source and full-duplex relay, AEU-International Journal of Electronics and Communications (2019) 152957.

[23] B. C. Nguyen, T. M. Hoang, P. T. Tran, Performance analysis of full-duplex decode-and-forward relay system with energy harvesting over nakagami-m fading channels, AEU-International Journal of Electronics and Communications 98 (2019) 114–122.

[24] Z. Hadzi-Velkov, N. Zlatanov, T. Q. Duong, R. Schober, Rate maximization of decode-and-forward relaying systems with RF energy harvesting, IEEE Communications Letters 19 (12) (2015) 2290–2293.

[25] W. Wu, X. Yin, P. Deng, T. Guo, B. Wang, Transceiver design for downlink SWIPT NOMA systems with cooperative full-duplex relaying, IEEE Access 7 (2019) 33464–33472.

[26] W. Wu, B. Wang, Z. Deng, H. Zhang, Secure beamforming for full-duplex wireless powered communication systems with self-energy recycling, IEEE Wireless Communications Letters 6 (2) (2016) 146–149.

[27] W. Wu, B. Wang, Y. Zeng, H. Zhang, Z. Yang, Z. Deng, Robust secure beamforming for wireless powered full-duplex systems with self-energy recycling, IEEE Transactions on Vehicular Technology 66 (11) (2017) 10055–10069.

[28] Q.-V. Pham, F. Fang, V. N. Ha, M. Le, Z. Ding, L. B. Le, W.-J. Hwang, A survey of multi-access edge computing in 5G and beyond: Fundamentals, technology integration, and state-of-the-art, arXiv preprint arXiv:1906.08452.

[29] N. H. Mahmood, H. Alves, O. A. López, M. Shehab, D. P. M. Osorio, M. Latva-aho, Six key enablers for machine type communication in 6G, arXiv preprint arXiv:1903.05406.

[30] G. Liu, F. R. Yu, H. Ji, V. C. Leung, X. Li, In-band full-duplex relaying: A survey, research issues and challenges, IEEE Communications Surveys & Tutorials 17 (2) (2015) 500–524.

[31] Y. Ai, M. Cheffena, A. Mathur, H. Lei, On physical layer security of double rayleigh fading channels for vehicular communications, IEEE Wireless Communications Letters.

[32] T. T. Duy, G. C. Alexandropoulos, V. T. Tung, V. N. Son, T. Q. Duong, Outage performance of cognitive cooperative networks with relay selection over double-rayleigh fading channels, IET Communications 10 (1) (2016) 57–64.

[33] P. S. Bithas, K. Maliatsos, A. G. Kanatas, V2V communication systems under correlated double-rayleigh fading channels, in: Vehicular Technology Conference (VTC Spring), 2016 IEEE 83rd, IEEE, 2016, pp. 1–5.

[34] A. Sabharwal, P. Schniter, D. Guo, D. W. Bliss, S. Rangarajan, R. Wichman, In-band full-duplex wireless: Challenges and opportunities, IEEE J. Sel. Areas in Commun. 32 (9) (2014) 1637–1652. doi:10.1109/JSAC.2014.2330193.

[35] X. Lu, P. Wang, D. Niyato, D. I. Kim, Z. Han, Wireless networks with RF energy harvesting: A contemporary survey, IEEE Communications Surveys Tutorials 17 (2) (2015) 757–789. doi:10.1109/COMST.2014.2368999.

[36] B. Clerckx, R. Zhang, R. Schober, D. W. K. Ng, D. I. Kim, H. V. Poor, Fundamentals of wireless information and power transfer: From RF energy harvester models to signal and system designs, IEEE Journal on Selected Areas in Communications 37 (1) (2018) 4–33.

[37] Y. Dong, M. J. Hossain, J. Cheng, Performance of wireless powered amplify and forward relaying over nakagami-m fading channels with nonlinear energy harvester, IEEE Communications Letters 20 (4) (2016) 672–675.

[38] C. Zhong, H. A. Suraweera, G. Zheng, I. Krikidis, Z. Zhang, Wireless information and power transfer with full duplex relaying, IEEE Transactions on Communications 62 (10) (2014) 3447–3461.

[39] B. C. Nguyen, X. N. Tran, D. T. Tran, L. T. Dung, Full-duplex amplify-and-forward relay system with direct link: Performance analysis and optimization, Physical Communication (2019) 100888.

[40] X. N. Tran, B. C. Nguyen, D. T. Tran, Outage probability of two-way full-duplex relay system with hardware impairments, in: 2019 3rd International Conference on Recent Advances in Signal Processing, Telecommunications & Computing (SigTelCom), IEEE, 2019, pp. 135–139.

[41] L. V. Nguyen, B. C. Nguyen, X. N. Tran, L. T. Dung, Transmit antenna selection for full-duplex spatial modulation multiple-input multiple-output system, IEEE Systems Journal.

[42] A. Goldsmith, Wireless communications, Cambridge university press, 2005.

[43] A. Jeffrey, D. Zwillinger, Table of integrals, series, and products, Academic press, 2007.

[44] A. S. Akki, F. Haber, A statistical model of mobile-to-mobile land communication channel, IEEE transactions on vehicular technology 35 (1) (1986) 2–7.

[45] I. Kovacs, Radio channel characterisation for private mobile radio systems - mobile-to-mobile radio link investigations: Mobile-to-mobile radio link investigations, Ph.D. thesis (2002).

[46] J. Salo, H. M. El-Sallabi, P. Vainikainen, Impact of double-rayleigh fading on system performance, in: 2006 1st International Symposium on Wireless Pervasive Computing, 2006, pp. 5 pp.–5. doi:10.1109/ISWPC.2006.1613574.

[47] F. B. Hildebrand, Introduction to numerical analysis, Courier Corporation, 1987.